FLUORESCENCE RECOVERY SPECTROSCOPY AS A PROBE OF SLOW ROTATIONAL MOTIONS

WILLIAM A. WEGENER
Baylor University Medical Research Institute, Dallas, Texas 75246

ABSTRACT Pump-and-probe techniques can be used to follow the slow rotational motions of fluorescent labels bound to macromolecules in solution. A strong pulse of polarized light initially anisotropically depletes the ground-state population. A continuous low-intensity beam of variable polarization then probes the anisotropic ground-state distribution. Using an additional emission polarizer, the generated fluorescence can be recorded as it rises towards its prepump value. A general theory of fluorescence recovery spectroscopy (FRS) is presented that allows for irreversible depletion processes like photobleaching as well as slowly reversible processes like triplet formation. In either case, rotational motions modulate recovery through cosine-squared laws for dipolar absorption and emission processes. Certain pump, probe, and emission polarization directions eliminate the directional dependence of either dipole and simplify the resulting expressions. Two anisotropy functions can then be constructed to independently monitor the rotations of either dipole. These functions are identical in form to the anisotropy used in fluorescence depolarization measurements and all rotational models developed there apply here with minor modifications. Several setups are discussed that achieve the necessary polarization alignments. These include right-angle detection equipment that is commonly available in laboratories using fluorescence methods.

INTRODUCTION

Within the past decade many applications of fluorescence photobleaching recovery (FPR) have been used in order to follow translational motions of fluorescently labeled particles. Most of these studies involve lateral diffusion in synthetic or biological membranes and have been reviewed by Peters (1981). However, photobleaching by polarized light can create an initially anisotropic distribution in which fluorophores that have absorption dipoles along the exciting direction are preferentially destroyed. Smith et al. (1981*a*) bleached an entire spherical lipid vesicle along one direction and determined its radius from the time it took translational motion over the surface to reorient the long axis of lipid labels. With spot bleaching, the local orientational anisotropy can be probed by varying the polarization direction of the bleach relative to the subsequent low level illumination used to generate the fluorescence signal. Smith et al. (1981*b*) used the decay of this anisotropy to monitor slow rotational motions of a lipid probe below the membrane transition temperature.

Although an irreversible process like photobleaching allows one to measure recovery dynamics over indefinitely long times, the process of depletion by triplet formation lessens the occurrence of unwanted photochemistry and can be used over microsecond and millisecond time scales that are typical of triplet-state lifetimes. There are several ways to use triplet lifetimes in rotational relaxation experiments. All use a brief pulse or linearly polarized light to preferentially promote those chromophores that have absorption dipoles along the polarization direction into the excited triplet state. Cherry (1979) has reviewed methods involving transient linear absorption dichroism. A weak linear polarized beam passes through the sample with its polarization direction parallel or perpendicular to that of the pulse. Depending on the wavelengths, one can monitor anisotropic absorption from either the depleted ground state or the excited state. This approach has recently been used to follow rotational motions of several membrane constituents including oligosaccharide chains (Cherry et al., 1980) and bacteriorhodopsin (Cherry and Godfrey, 1981), and to follow elastic twisting and bending motions in double-stranded DNA that is either free in solution (Hogan et al., 1982) or is wrapped around nucleosome core particles (Wang et al., 1982).

Another triplet approach directly monitors the polarization of the phosphorescence emitted from the excited-state decay. Phosphorescence anisotropy measurements have been recently applied to membrane systems by several groups (Austin et al., 1979; Jovin et al., 1981) and the intrinsic phosphorescence of tryptophan has been used to monitor slow rotations of proteins (Strambini and Galley, 1980).

The most recent and most sensitive method applies the fact that under anaerobic conditions many labels, including the widely used eosin and tetramethylrhodamine, actively fluorescence and can be inactivated in sizeable numbers by being pumped into long-lived triplet states. Termed "depolarization of fluorescence depletion" by Johnson and Garland (1981), their method measures ground-state absorption anisotropy, not directly by mea-

suring absorption differences in a weak polarized probe beam, but indirectly by measuring the differences in the fluorescence intensity generated by anisotropic absorption and emission. They estimated that the sensitivity of this technique is many orders of magnitude below that of previous techniques using triplet lifetimes, and they were able to measure rotational relaxation of the band 3 protein on a single erythrocyte ghost using a spot that illuminated fewer than 1,000 copies of the protein.

Regardless of the depletion mechanisms, fluorescence recovery spectroscopy (FRS) appears to be a potentially powerful technique for monitoring slow rotational motions of large biological systems. Although some generalizations to oriented systems are immediately possible, the theory of FRS developed here applies only to randomly ordered systems such as suspensions of macromolecules, macromolecular complexes, membrane fragments, etc. As usual, the optical properties of a label are represented by several transition dipoles. Even so, a general FRS description of rotational dynamics still appears to be too complex to be useful because the FRS signal reflects both the anisotropic absorption and emission properties that result as a weak probe beam stimulates fluorescence. In contrast, linear absorption dichroism measurements involve only anisotropic absorption, and phosphorescence depolarization measurements involve only anisotropic emission.

Wegener and Rigler (1984) showed how simplifications occur in FPR setups for monitoring rotations when all the emitted fluorescent photons are collected without bias. Parabolic reflectors or integrating spheres using 2π or 4π collection optics can give FRS signals that depend on absorption, and not on emission dipole orientations. However, laboratories using fluorescence and phosphorescence methods for solution studies more commonly use small-angle collection optics. In a typical setup, a laser beam illuminates a solution contained in a rectangular cuvette and luminescence emitted along an axis at right angles passes through a small aperature in front of a photomultiplier.

As shown here, FRS setups using small-angle collection and polarizers can also give signals that depend only on absorption dipole orientations. In addition, signals can be obtained that depend only on emission dipole orientations. That is, by selective elimination, one can independently monitor two different rotational motions of a label if its transition dipoles for probe beam absorption and for fluorescence emission are different. Furthermore, the pump and probe beam wavelengths may be independently varied to stimulate different absorption dipoles. These freedoms may be particularly useful in anisotropic circumstances, such as those that occur with elongated polymers or membrane fragments, where different axes may rotate in highly different manners. Several setups are described for achieving the needed polarization configurations.

The paper then addresses the information available in the resulting FRS signals. For given pump and probe wavelengths, all nonorientational information concerning the labels is contained within one sum function, whereas all orientational information is contained within two anisotropy functions. These functions can be isolated from pairs of measurements where two polarization directions are parallel or perpendicular to each other. Assuming that translational relaxation is negligible during the time needed to complete rotational relaxation, the sum function monitors the replenishment of fluorescent labels as the fluorescently inactive state decays. The anisotropy functions each have the same form as in fluorescence depolarization and for rigid-body rotational diffusion involve up to five exponentials. The paper concludes by using a simple wobble model that qualitatively allows for rapid label motions at a binding site that cannot be resolved on time scales appropriate to this technique.

FRS Signal Dependence on Current Ground State Distribution

In this version of FRS, a solution of fluorescently labeled material is initially perturbed by a brief high-intensity pulse of light polarized along unit vector $\hat{\mathbf{p}}$. The pulse depletes the ground-state population by pumping the labels into some other state devoid of fluorescent activity. The nonfluorescent state may be an excited triplet state, a permanent state as in irreversible photobleaching, or any other state that is longlived compared with the fluorescent lifetime. The anisotropic ground-state distribution initially created by the pump pulse is then probed as a function of time by a weak, continuous beam polarized along unit vector $\hat{\mathbf{a}}$. It is assumed that the beam intensity is low enough to neglect its effect on the ground-state distribution. The fluorescence stimulated by the probe beam is recorded along some axis using a pinhole detector and an emission polarizer along unit vector $\hat{\mathbf{e}}$. Assuming that changes in the ground-state distribution are slow compared with fluorescent lifetimes, we ignore any delay between absorption of a probe photon and reemission of a fluorescent photon.

We now assume one species of label is present whose directional properties for light absorption and fluorescence emission involve transition dipoles. These dipoles are represented by unit vectors $\hat{\boldsymbol{\mu}}_a$ and $\hat{\boldsymbol{\mu}}_e$ fixed in the label, such that $(\hat{\boldsymbol{\mu}}_a \cdot \hat{\mathbf{a}})^2$ is the relative probability of absorbing a probe photon polarized along $\hat{\mathbf{a}}$ and $(\hat{\boldsymbol{\mu}}_e \cdot \hat{\mathbf{e}})^2$ is the relative probability of emitting a fluorescent photon polarized along $\hat{\mathbf{e}}$. Different absorption dipoles may be involved if the pump and probe beams have different wavelengths. To allow for this simply, we let $\hat{\boldsymbol{\mu}}_p$ be another unit vector fixed in the label such that $(\hat{\boldsymbol{\mu}}_p \cdot \hat{\mathbf{p}})^2$ is the relative probability of absorbing a pump photon polarized along $\hat{\mathbf{p}}$. Generally, no special relation is assumed between $\hat{\boldsymbol{\mu}}_a$, $\hat{\boldsymbol{\mu}}_e$, and $\hat{\boldsymbol{\mu}}_p$. If ω denotes Euler coordinate or any other three coordinates needed to specify a label's orientation relative to laboratory axes, then $\hat{\boldsymbol{\mu}}_a(\omega)$, $\hat{\boldsymbol{\mu}}_e(\omega)$, and $\hat{\boldsymbol{\mu}}_p(\omega)$ indicate the functional dependencies of these vectors on label orientation ω.

Let $R(\hat{\mathbf{p}}, \mathbf{r}, \omega, t)\mathrm{d}^3\mathbf{r}\mathrm{d}^3\omega$ be the number of labels in the ground state at time t positions within $\mathrm{d}^3\mathbf{r}$ about $\mathbf{r}$ and orientations within $\mathrm{d}^3\omega$ about ω following a pump pulse at $t = 0$ polarized along $\hat{\mathbf{p}}$. The distribution is normalized such that integration overall $8\pi^2$ orientations gives the number concentration $n(\mathbf{r}, t)$ of ground-state labels at position $\mathbf{r}$ at time t. The probe beam is constant in time with intensity $I(\mathbf{r})$ at each position. If $Q = Q(\omega)$ is some function of label orientation, then its mean-probed value at time t, denoted $\overline{Q}$, is defined by averaging the ground-state distribution weighted by $I(\mathbf{r})$ overall orientations and positions at that time according to

$$\overline{Q} = \iint I(\mathbf{r})Q(\omega)R(\hat{\mathbf{p}}, \mathbf{r}, \omega, t)\,\mathrm{d}^3\mathbf{r}\mathrm{d}^3\omega. \quad (1)$$

With this definition, the recorded fluorescence signal F at time t is given as

$$F(t) = 9q\overline{(\hat{\boldsymbol{\mu}}_a \cdot \hat{\mathbf{a}})^2(\hat{\boldsymbol{\mu}}_e \cdot \hat{\mathbf{e}})^2}, \quad (2)$$

where q is a product of the label's quantum efficiencies for probe absorption, fluorescence emission, and detection. As shown below, the factor 9 accounts for the fact that isotropically averaged values of $(\hat{\boldsymbol{\mu}}_a \cdot \hat{\mathbf{a}})^2$ and $(\hat{\boldsymbol{\mu}}_e \cdot \hat{\mathbf{e}})^2$ are $1/3$. Although Eq. 2 explicitly displays the angular dependence of F on the probe polarization and emission polarizer, the dependence on the pump polarization $\hat{\mathbf{p}}$ used to align the initial ground-state distribution, is implied from the definition of the mean-probed value given in Eq. 1.

Reduction of FRS Signal to Simpler Forms $A(t)$ and $E(t)$

The initially created anisotropic distribution will recover its isotropic character as the labels undergo rotational diffusion, and different aspects of this recovery can be monitored by varying the three polarization directions $\hat{\mathbf{p}}$, $\hat{\mathbf{a}}$, and $\hat{\mathbf{e}}$. Aragon and Pecora (1975) showed that if all emitted photons were collected equally (instead of only detecting emitted photons along a particular axis with a particular polarization) then the cosine-squared term involving $\hat{\boldsymbol{\mu}}_e$ would not be present in the fluorescence signal. Similarly, we could imagine another situation in which the sample is probed without polarization bias and the cosine-squared term involving $\hat{\boldsymbol{\mu}}_a$ would not be present in the fluorescence signal.

Anticipating these situations, we define A and E as

$$A(t) = 3q\overline{(\hat{\boldsymbol{\mu}}_a \cdot \hat{\mathbf{a}})^2}, \quad E(t) = 3q\overline{(\hat{\boldsymbol{\mu}}_e \cdot \hat{\mathbf{e}})^2}; \quad (3)$$

and let $A_\parallel$ and $A_\perp$ denote special cases of A with $\hat{\mathbf{a}} \cdot \hat{\mathbf{p}} = \pm 1$ and $\hat{\mathbf{a}} \cdot \hat{\mathbf{p}} = 0$, respectively, whereas $E_\parallel$ and $E_\perp$ denote special cases of E with $\hat{\mathbf{e}} \cdot \hat{\mathbf{p}} = \pm 1$ and $\hat{\mathbf{e}} \cdot \hat{\mathbf{p}} = 0$, respectively. Generally, of the three polarization directions $\hat{\mathbf{p}}$, $\hat{\mathbf{a}}$, and $\hat{\mathbf{e}}$, no choice exists that reduces F to A or E for all times following the pump pulse. However, as we now show, for special cases where two polarization directions are aligned parallel or perpendicular to each other, the third direction can be chosen from symmetry considerations so that all four cases $A_\parallel$, $A_\perp$, $E_\parallel$, and $E_\perp$ can be experimentally realized.

As discussed below, in all practical cases, $R(\hat{\mathbf{p}}, \mathbf{r}, \omega, t)$ has cylindrical symmetry about $\hat{\mathbf{p}}$ at each position $\mathbf{r}$ that is independent of time t. For $A_\parallel$, we note that $R(\hat{\mathbf{p}}, \mathbf{r}, \omega, t)(\hat{\boldsymbol{\mu}}_a \cdot \hat{\mathbf{p}})^2$ is cylindrically symmetric about $\hat{\mathbf{p}}$. If $\hat{\mathbf{e}}$ is tilted by angle θ_e from $\hat{\mathbf{p}}$ towards some unit vector $\hat{\mathbf{n}}$ perpendicular to $\hat{\mathbf{p}}$, then $(\hat{\boldsymbol{\mu}}_e \cdot \hat{\mathbf{e}})^2$, in Eq. 2, can be replaced by

$$\cos^2\theta_e(\hat{\boldsymbol{\mu}}_e \cdot \hat{\mathbf{p}})^2 + \sin^2\theta_e(\hat{\boldsymbol{\mu}}_e \cdot \hat{\mathbf{n}})^2,$$

because the additional $\sin\theta_e\cos\theta_e$ cross term vanishes upon integration. At the magic angle 54.7°, $\cos^2\theta_e = 1/3$, the expansion collapses to $1/3$ and F reduces to $A_\parallel$ as desired. For $A_\perp$, we note that when $\hat{\mathbf{a}} \cdot \hat{\mathbf{p}} = 0$, $R(\hat{\mathbf{p}}, \mathbf{r}, \omega, t)(\hat{\boldsymbol{\mu}}_a \cdot \hat{\mathbf{a}})^2$ has three orthogonal planes of reflection symmetry that are time independent: the plane normal to $\hat{\mathbf{p}}$, the plane spanned by $\hat{\mathbf{p}}$ and $\hat{\mathbf{a}}$, and the plane spanned by $\hat{\mathbf{p}}$ and $\hat{\mathbf{a}} \times \hat{\mathbf{p}}$. The vectors $\hat{\mathbf{p}}$, $\hat{\mathbf{a}}$, and $\hat{\mathbf{a}} \times \hat{\mathbf{p}}$ lie along three principal axes and we can expand $(\hat{\boldsymbol{\mu}}_e \cdot \hat{\mathbf{e}})^2$ in Eq. (2) as

$$(\hat{\boldsymbol{\mu}}_e \cdot \hat{\mathbf{a}})^2(\hat{\mathbf{a}} \cdot \hat{\mathbf{e}})^2 + (\hat{\boldsymbol{\mu}}_e \cdot \hat{\mathbf{p}})^2(\hat{\mathbf{p}} \cdot \hat{\mathbf{e}})^2 + (\hat{\boldsymbol{\mu}}_e \cdot \hat{\mathbf{a}} \times \hat{\mathbf{p}})^2(\hat{\mathbf{a}} \times \hat{\mathbf{p}} \cdot \hat{\mathbf{e}})^2,$$

because the cross terms vanish by symmetry upon integration. If $(\hat{\mathbf{a}} \cdot \hat{\mathbf{e}})^2 = (\hat{\mathbf{p}} \cdot \hat{\mathbf{e}})^2 = (\hat{\mathbf{a}} \times \hat{\mathbf{p}} \cdot \hat{\mathbf{e}})^2 = 1/3$, then this expansion collapses to $1/3$ and F reduces to $A_\perp$. The arguments for $E_\parallel$ and $E_\perp$ are completely analogous: if $(\hat{\mathbf{e}} \cdot \hat{\mathbf{p}})^2 = 1$, any $\hat{\mathbf{a}}$ tilted 54.7° from $\hat{\mathbf{p}}$ reduces F to $E_\parallel$, whereas if $\hat{\mathbf{e}} \cdot \hat{\mathbf{p}} = 0$, any $\hat{\mathbf{a}}$ satisfying $(\hat{\mathbf{a}} \cdot \hat{\mathbf{e}})^2 = (\hat{\mathbf{a}} \cdot \hat{\mathbf{p}})^2 = (\hat{\mathbf{a}} \cdot \hat{\mathbf{e}} \times \hat{\mathbf{p}})^2 = 1/3$ reduces F to $F_\perp$.

Setups for Measuring Parallel and Perpendicular Components of $A(t)$ and $E(t)$

Fig. 1 shows a simple setup for measuring all four special cases. The sample to be studied is located at the origin of laboratory axes x, y, and z, with z assumed to be vertical. Both beams propagate along y and fluorescence emission is detected along x. To obtain $A_\parallel$ and $A_\perp$, the pump is polarized 45° from the vertical and the emission polarizer in front of the detector is rotated 35.3° from the vertical. A probe beam polarized parallel (perpendicular) to the pump then gives $A_\parallel$ ($A_\perp$). To measure $E_\parallel$, the pump polarization direction and the emission polarizer are vertically aligned, while the probe beam is polarized 54.7° from the vertical. To measure $E_\perp$, the pump is horizontally polarized, the emission polarizer is 45° from the vertical, and the probe beam is polarized 35.3° from the vertical.

Although this setup uses only one beam path and right-angle detection, all three polarization directions must be switched from $E_\parallel$ to $E_\perp$. Fig. 2 shows an alternative setup using one beam path that requires minimal polarization switches. The sample is located at the center of x-, y-, and z-axes with z vertical. Both beams travel along y, and

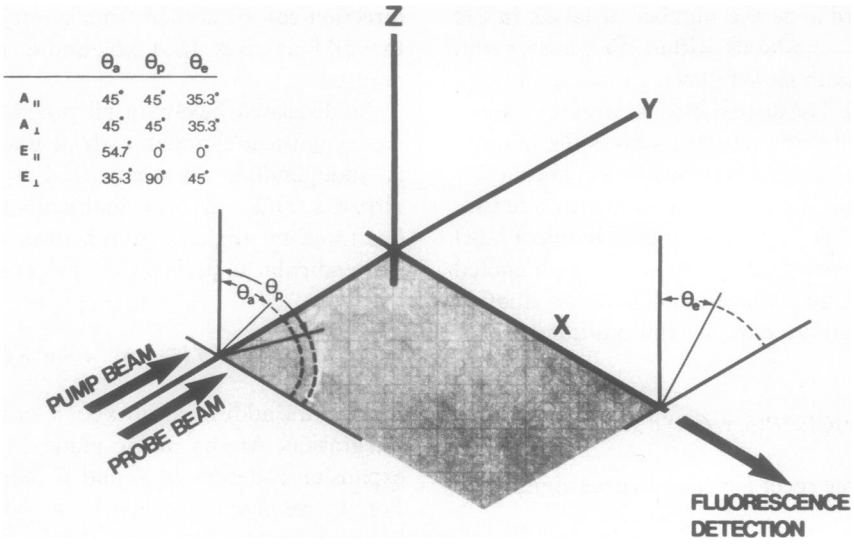

	θ_a	θ_p	θ_e
$A_{\parallel}$	45°	45°	35.3°
$A_{\perp}$	45°	45°	35.3°
$E_{\parallel}$	54.7°	0°	0°
$E_{\perp}$	35.3°	90°	45°

FIGURE 1 An FRS setup using one beam path and right-angle detection is shown. The sample is located at the center of the x-, y-, and z-axes with the z-axis assumed to be vertical. Pump and probe beams travel along the y-axis, with fluorescence detected along the x-axis. The pump and probe beams are linearly polarized at angles θ_p and θ_a from the vertical, respectively, while the fluorescence emission passes through a linear polarizer at angle θ_e from the vertical. The insert table shows four particular settings of these angles that give $A_{\parallel}$, $A_{\perp}$, $E_{\parallel}$, and $E_{\perp}$.

fluorescence emission is detected along an oblique axis midway between x and y. The pump pulse is vertically polarized. With the emission polarizer rotated 54.7° from the vertical, a probe beam polarized vertically (horizontally) gives $A_{\parallel}$ ($A_{\perp}$). With the probe beam polarized 54.7° from the vertical, an emission polarizer aligned vertically (horizontally) gives $E_{\parallel}$ ($E_{\perp}$).

Sometimes, it may be desirable to use separate beam paths. Fig. 3 shows a setup in which detection occurs at right angles to the propagation axis of the pump pulse, but

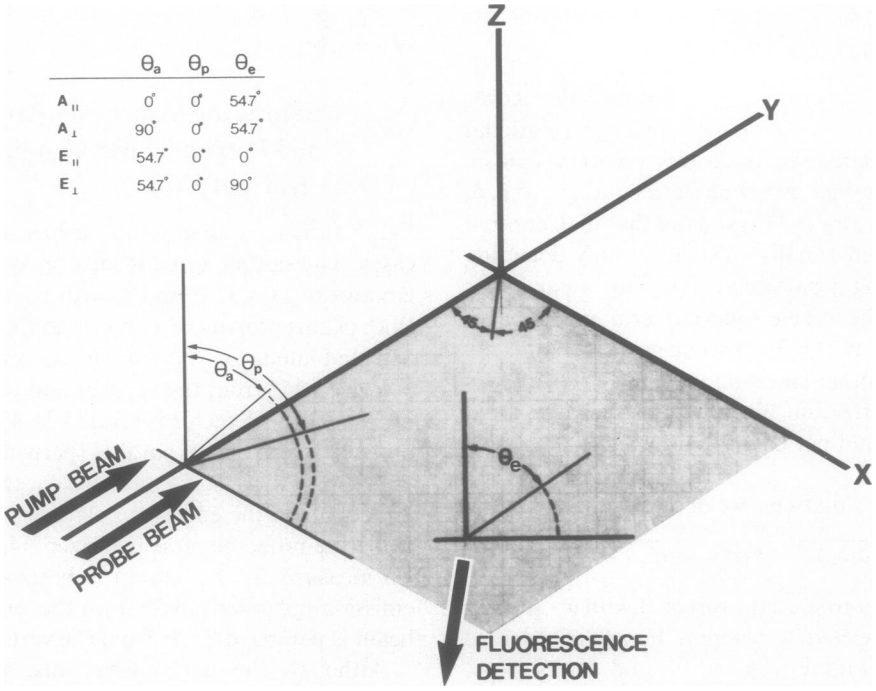

	θ_a	θ_p	θ_e
$A_{\parallel}$	0°	0°	54.7°
$A_{\perp}$	90°	0°	54.7°
$E_{\parallel}$	54.7°	0°	0°
$E_{\perp}$	54.7°	0°	90°

FIGURE 2 An FRS setup using one beam path and oblique detection is shown. The sample is located at the center of the x-, y-, and z-axes with the z-axis assumed to be vertical. Both beams propagate along the y-axis and fluorescence emission is detected along a horizontal axis midway between the x and y axes. The pump and probe beams are linearly polarized at angles θ_p and θ_a from the vertical, respectively, while the fluorescence emission passes through a linear polarizer at angle θ_e from the vertical. The insert table shows four particular settings of these angles that give $A_{\parallel}$, $A_{\perp}$, $E_{\parallel}$, and $E_{\perp}$.

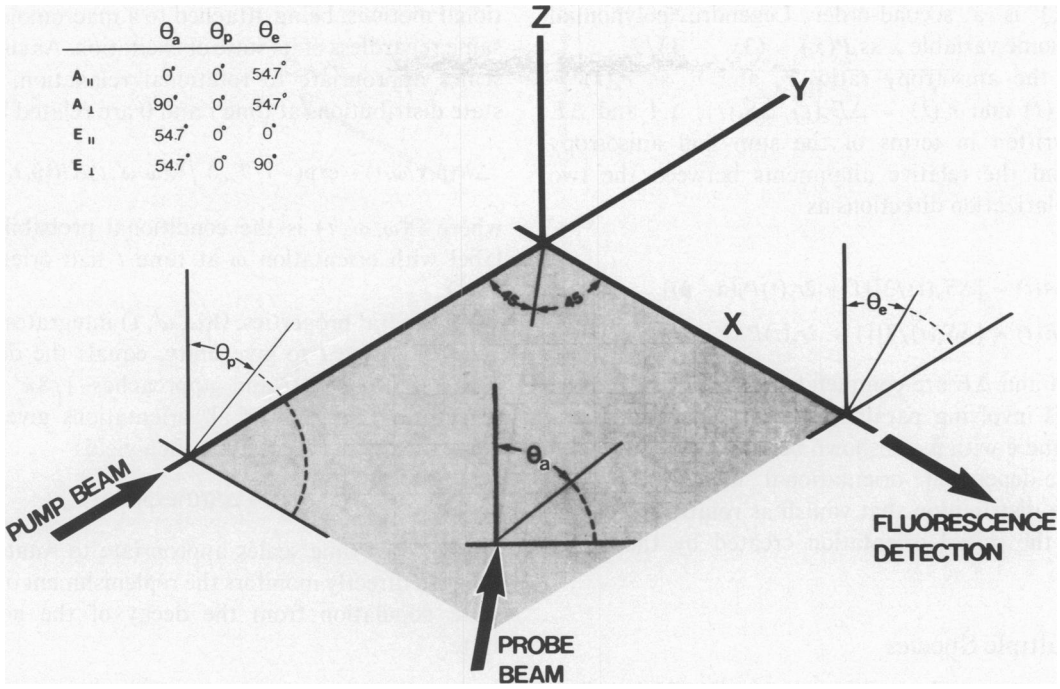

FIGURE 3 An FRS setup using separate beams paths is shown. The sample is located at the center of the x-, y-, and z-axes with the z-axis assumed to be vertical. The pump pulse propagates along the y-axis, the probe beam propagates horizontally along an axis midway between the x- and y-axes, and fluorescence emission is detected along the x-axis. The pump and probe beams are linearly polarized at angles θ_p and θ_a from the vertical, respectively, while the fluorescence emission passes through a linear polarizer at angle θ_e from the vertical. The insert table shows four particular settings of these angles that give $A_\parallel$, $A_\perp$, $E_\parallel$, and $E_\perp$.

the probe beam comes from an oblique angle. The sample is at the center of x-, y-, and z-axes with z vertical. The pump pulse is vertically polarized and travels along y, fluorescence is detected along x, and the pump beam travels along an axis midway between x and y. With the emission polarizer rotated 54.7° from the vertical, a probe beam polarized vertically (horizontally) gives $A_\parallel$ ($A_\perp$). With the probe beam polarized at 54.7° from the vertical, an emission polarizer aligned vertically (horizontally) gives values of $E_\parallel$ ($E_\perp$).

$A(t)$ and $E(t)$ Determined by Sum and Anisotropy Functions

The information available in $A(t)$ and $E(t)$ concerning the ground-state distribution can be obtained from the special cases involving parallel and perpendicular alignments. To discuss changes in fluorescence signal, we define the following: $\Delta A = A_0 - A$ and $\Delta E = E_0 - E$, where A_0 and E_0 denote prepump signals; $\Delta n(\mathbf{r}, t) = n_0 - n(\mathbf{r}, t)$, where n_0 is the prepump label concentration; and $\Delta R(\hat{\mathbf{p}}, \mathbf{r}, \omega, t) = n_0/8\pi^2 - R(\hat{\mathbf{p}}, \mathbf{r}, \omega, t)$ because $n_0/8\pi^2$ is the prepump isotropic distribution. Because the pump depletes the ground state, ΔA, ΔE, $\Delta R(\hat{\mathbf{p}}, \mathbf{r}, \omega, t)$ and $\Delta n(\mathbf{r}, t)$ are expected to be positive quantities that decrease towards zero as recovery processes occur. From Eq. 2, A_0 and E_0 are identical and are given as $qn_0 \int I(\mathbf{r})d^3\mathbf{r}$, with the integral extending only over the sample region illuminated by the probe.

Because the system was originally randomly oriented, the pump pulse creates a ground-state distribution with initial cylindrical symmetry about $\hat{\mathbf{p}}$. We assume that orientational relaxation is completed while the label remains in a small neighborhood about its initial position over which $I(\mathbf{r})$ and $R(\hat{\mathbf{p}}, \mathbf{r}, \omega, t)$ are constant. For freely diffusing macromolecules, the neighborhood typically extends several particle lengths, over which spatial gradients in typical pump and probe beams are completely negligible. Hence, the distribution maintains cylindrical symmetry about $\hat{\mathbf{p}}$ for all times because the only possible symmetry-breaking mechanism, involving spatial gradient effects during rotational relaxation, can be ignored.

To isolate the nonrotational contributions in $\Delta A(t)$ and $\Delta E(t)$, we consider the sum combinations $\Delta S_a = \Delta A_\parallel + 2\Delta A_\perp$ and $\Delta S_e = \Delta E_\parallel + 2\Delta E_\perp$. From cylindrical symmetry about $\hat{\mathbf{p}}$, ΔS_a and ΔS_e are equal and denoted ΔS, where

$$\Delta S(t) = 3q \int I(\mathbf{r})\Delta n(\mathbf{r}, t)d^3\mathbf{r} \tag{4}$$

involves only the concentration difference weighted by the beam intensity. Expanding $\Delta n(\mathbf{r}, t)$ in Eq. 4, we can also write $\Delta S = S_0 - S$, where S_0 is the prepump value of $S = A_\parallel + 2A_\perp = E_\parallel + 2E_\perp$.

To isolate the rotational contributions, we first consider the difference combinations $\Delta D_a = \Delta A_\parallel - \Delta A_\perp$ and $\Delta D_e = \Delta E_\parallel - \Delta E_\perp$. From cylindrical symmetry about $\hat{\mathbf{p}}$,

$$\Delta D_a(t) = 3q\overline{P_2(\hat{\mu}_a \cdot \hat{\mathbf{p}})}; \qquad \Delta D_e(t) = 3q\overline{P_2(\hat{\mu}_e \cdot \hat{\mathbf{p}})}, \tag{5}$$

where $P_2(x)$ is a second-order Legendre polynomial defined for some variable x as $P(x) = (3x^2 - 1)/2$.

Defining the anisotropy ratios r_a and r_e as $r_a(t) = \Delta D_a(t)/\Delta S_a(t)$ and $r_e(t) = \Delta D_e(t)/\Delta S_e(t)$, ΔA and ΔE can be rewritten in terms of the sum and anisotropy functions and the relative alignments between the two pertinent polarization directions as

$$\Delta A(t) = [\Delta S_a(t)/3][1 + 2r_a(t)P_2(\hat{\mathbf{a}} \cdot \hat{\mathbf{p}})]$$
$$\Delta E(t) = [\Delta S_e(t)/3][1 + 2r_e(t)P_2(\hat{\mathbf{e}} \cdot \hat{\mathbf{p}})]. \quad (6)$$

As seen, ΔA and ΔE are completely determined from the special cases involving parallel and perpendicular alignments of $\hat{\mathbf{a}}$ and $\hat{\mathbf{e}}$ with $\hat{\mathbf{p}}$. As shown below, the ratios r_a and r_e are time-dependent orientational moments of the ground-state distribution that vanish as rotational relaxation erases the initial orientation created by the pump pulse.

Multiple Species

Although Eqs. 6 were derived for one species of label, they are general relations that apply if the sample contains several species, because fluorescence emission intensities are additive. As before, $\Delta S_a = \Delta S_e = \Delta S$, and the observed ΔS can be written

$$\Delta S(t) = \sum_i \Delta S^i(t), \quad (7)$$

with ΔS^i given by Eq. 4 for each species i. The observed anisotropy ratios r_a and r_e can be expressed as

$$r_a(t) = \sum_i \Delta S^i(t) r_a^i(t)/\Delta S(t),$$
$$r_e(t) = \sum_i \Delta S^i(t) r_e^i(t)/\Delta S(t); \quad (8)$$

with $r_a^i(t) = \Delta D_a(t)/\Delta S^i(t)$, $r_e^i(t) = \Delta D_e(t)/\Delta S^i(t)$, and ΔD_a^i, ΔD_e^i given by Eq. 5 for each species i. Note that in case of multiple species, the relative contribution of each species to the total anisotropy functions involves a fractional weighting term that may introduce an additional source of time dependence.

Expressions for a Single Species Undergoing Rotational Diffusion

The simplest case of solution dynamics involves free diffusion of a single species. We consider an infinitely dilute, noninteracting solution of identical macromolecules specifically labeled uniquely at one site. As previously discussed, we assume that rotational relaxation occurs without significant changes in position compared with any spatial gradients related to the pump or probe beams. We also assume that the nonfluorescent state decays to the ground state exponentially with lifetime T_{exc} and that the label's rotational motions, being attached to a macromolecule, are the same regardless of its state of excitation. As such, over time scales appropriate to rotational relaxation, the ground-state distributions at time t and 0 are related by

$$\Delta R(\hat{\mathbf{p}}, \mathbf{r}, \omega, t) = \exp(-t/T_{exc}) \int \Omega(\omega, \omega', t) \Delta R(\hat{\mathbf{p}}, \mathbf{r}, \omega, 0) d^3\omega', \quad (9)$$

where $\Omega(\omega, \omega', t)$ is the conditional probability that any label with orientation ω at time t had orientation ω' at $t = 0$.

As general properties, $\Omega(\omega, \omega', t)$ integrates over all ω or ω' at any time t to give unity, equals the delta function $\delta(\omega, \omega')$ at $t = 0$, and approaches $1/8\pi^2$ as $t \rightarrow \infty$. Integrating Eq. 9 over all orientations gives $\Delta n(\mathbf{r}, t) = \Delta n(\mathbf{r}, 0)\exp(-t/T_{exc})$. Eq. 4 then yields

$$\Delta S(t) = \Delta S(0)\exp(-t/T_{exc}). \quad (10)$$

Hence, over time scales appropriate to rotational relaxation, ΔS directly monitors the replenishment of the ground-state population from the decay of the nonfluorescent state.

Rotational Dynamics and Anisotropy Functions

To consider rotational dynamics we now explicitly assume that the brief pump pulse is a delta function so that our results formally constitute impulse response functions. Because the labels are completely random before the pulse, the ground-state ensemble with a particular $\hat{\boldsymbol{\mu}}_p$, instantaneously formed at $t = 0$, has a distribution of $\hat{\boldsymbol{\mu}}_a$ or $\hat{\boldsymbol{\mu}}_e$ cylindrically symmetric about this direction. For solution systems undergoing rotational diffusion without any preferred external axes, there is no mechanism to destroy this symmetry, and this ensemble retains a cylindrically symmetric distribution of $\hat{\boldsymbol{\mu}}_a$ and $\hat{\boldsymbol{\mu}}_e$ about the original $\hat{\boldsymbol{\mu}}_p$ direction as it evolves. Furthermore, the nature of the evolution must be the same, regardless of which particular $\hat{\boldsymbol{\mu}}_p$ was involved, because the conditional probability that a label moves from one orientation to another in time t can only depend on the relative difference between them.

Following Kinosita et al. (1977), these properties allow us to cleanly separate the rotational dynamics from the initial conditions in ΔD_a and ΔD_e, without having to specify a rotational model first. The results can be expressed as the product of three terms. The first term is simply $\exp(-t/T_{exc})$. The second term is the same in both cases and contains the dependence on the initial alignment at $t = 0$ achieved by the pump pulse. If we define ΔD_p involving the pump absorption dipole analogously to the difference functions defined for the other dipoles so $\Delta D_p(t) = 3qP_2(\hat{\boldsymbol{\mu}}_p \cdot \hat{\mathbf{p}})$, then this second term is simply $\Delta D(0)_p$. The other terms are expectation values of second-order Legendre polynomials involving dot products between the $\hat{\boldsymbol{\mu}}_p$ vector that a label has at $t = 0$ and either its $\hat{\boldsymbol{\mu}}_a$ or $\hat{\boldsymbol{\mu}}_e$

vector at time t. These expectation values are denoted $\langle P_2[\hat{\mu}_a(t) \cdot \hat{\mu}_p(0)] \rangle$ and $\langle P_2[\hat{\mu}_e(t) \cdot \hat{\mu}_p(0)] \rangle$, respectively, and are defined in terms of label orientations and conditional probabilities as

$$\langle P_2[\hat{\mu}_a(t) \cdot \hat{\mu}_p(0)] \rangle = \int P_2(\hat{\mu}_a(\omega) \cdot \hat{\mu}_p(\omega')] \, \Omega(\omega, \omega', t) \, d^3\omega$$

$$\langle P_2[\hat{\mu}_e(t) \cdot \hat{\mu}_p(0)] \rangle = \int P_2(\hat{\mu}_e(\omega) \cdot \hat{\mathbf{m}}_p(\omega')] \, \Omega(\omega, \omega', t) \, d^3\omega \tag{11}$$

with any choice of initial orientation ω' giving the same results for an unoriented system.

Using $\Delta S(t)$, the dependence on the rate of ground-state repopulation cancels and we obtain

$$r_a(t) = g_0 \langle P_2[\hat{\mu}_a(t) \cdot \hat{\mu}_p(0)] \rangle;$$

$$r_e(t) = g_0 \langle P_2[\hat{\mu}_e(t) \cdot \hat{\mu}_p(0)] \rangle, \tag{12}$$

where $g_0 = \Delta D_p(0)/\Delta S(0)$ is a simple constant that we later show reduces to 2/5 for sufficiently low pump strengths. As seen, $r_a(t)$ and $r_e(t)$ express average values involving dot products between a label's original $\hat{\mu}_p$ and its current $\hat{\mu}_a$ and $\hat{\mu}_e$, respectively. These functions thus monitor different average rotational motions of the label. If $g_0 = 2/5$, they are identical in form to the anisotropy in fluorescence depolarization (Wahl, 1975; Kinosita et al., 1977), so that dynamic rotational models developed elsewhere can be applied here with minor modifications.

Let δ_a and δ_e denote the angles that $\hat{\mu}_a$ and $\hat{\mu}_e$ make with $\hat{\mu}_p$ in the label's fixed molecular axes. For a label rigidly fixed to a sphere with rotational diffusion coefficient D,

$$r_a(t) = g_0 P_2(\cos\delta_a)\exp(-6Dt),$$

$$r_e(t) = g_0 P_2(\cos\delta_e)\exp(-6Dt), \tag{13}$$

in which case both functions exhibit the same time dependence although their initial values may be quite different. If either of the two unit vectors lies along a symmetry axis of a body of revolution, the anisotropy functions involved also have the same form, with D being the end-over-end diffusion coefficient. In the more general case of a label firmly fixed to an arbitrary rigid body, the expressions are complicated and involve five exponentials, although only three are distinct if there is an axis of revolution (Ehrenberg and Rigler, 1972; Chuang and Eisenthal, 1972; Belford et al., 1972).

Initial Values

The initial values of the sum and anisotropy functions reflect the initial distribution created by the pump as well as the degree of overlap between the pump and probe beams. To qualitatively examine a variety of pump conditions, we assume the pump intensity $I_p(\mathbf{r})$ at each position $\mathbf{r}$ is constant over period T. Picking positions so that the maximum intensity occurs at $\mathbf{r} = 0$, we define $f(\mathbf{r}) = I_p(\mathbf{r})/I_p(0)$. A label at position $\mathbf{r}$ with orientation ω is inactivated at the instantaneous rate $3q_pI_p(0)f(\mathbf{r})[\hat{\mu}_p(\omega) \cdot \hat{\mathbf{p}}]^2$, where q_p is a product of the label's quantum efficiencies involved in the process. The degree of pumping achieved by the pulse is then characterized by a parameter K, where $K = q_pTI_p(0)$, and if the label's $\hat{\mu}_p$ does not rotate during the pump pulse, the initial distribution is

$$R(\hat{\mathbf{p}}, \mathbf{r}, \omega, 0) = R_0\exp[-3Kf(\mathbf{r})[\hat{\mu}_p(\omega) \cdot \hat{\mathbf{p}}]^2], \tag{14}$$

with $n(\mathbf{r}, 0)$ following by integration over $8\pi^2$.

If the probe beam intersects regions of the sample solution not illuminated by the pump pulse, the fluorescence signal will contain some unwanted background. So far we have eliminated this background in our analysis by using changes in fluorescence signal such as ΔA and ΔE. However, because the changes obtained in an experiment are themselves likely to be small, this background should be as small as possible. To qualitatively describe this efficiency, we introduce an overlap function s

$$s = \int I(\mathbf{r})f(\mathbf{r})d^3\mathbf{r} / \int I(\mathbf{r})d^3\mathbf{r}, \tag{15}$$

in which the integrals are restricted to the sample solution. If the probe beam intersects only pumped regions, s is of the order unity. For coincident beam paths with Gaussian intensity profiles of the same width, $s = 1/2$. However, in a mismatched arrangement s could be much smaller. For uniform intensity beams, $s = v/V$, where v is the solution volume in which the beams overlap and V is the solution volume occupied by the probe beam. As we shall now show, the most useful analytic results involve the regime of small pumping for which $K \ll 1$. However, in this regime fluorescence signal changes are linearly proportional to the product Ks and not just K.

Expanding $R(\hat{\mathbf{p}}, \mathbf{r}, \omega, t)$ as a Taylor series in K, we obtain

$$\Delta S(0)/S_0 = sK[1 - (9/10)s'K + \ldots]$$

$$\Delta D(0)_p/S_0 = (2/5)sK[1 - (9/7)s'K + \ldots] \tag{16}$$

where s' is obtained by replacing $I(\mathbf{r})$ by $I(\mathbf{r})f(\mathbf{r})$ in Eq. 15. For coincident laser beams with Gaussian intensity profiles, $s' = 2/3$. For uniform intensity beams, $s' = 1$, regardless of the degree of overlap. By construction, s' remains of the order unity even for mismatched beams. As seen, signal changes are proportional to sK at small K, with the next correction terms indicated.

Taking the ratio $\Delta D(0)_p/\Delta S(0)$ gives

$$g_0 = 2/5[1 - (27/70)s'K + \ldots]. \tag{17}$$

Hence, to first order in K, $g_0 = 2/5$, regardless of the detailed nature of the pump or probe patterns or their degree of overlap. At higher K, g_0 gradually decreases towards zero and the first correction term is given.

Rotational motion during the pump period will give

initial anisotropy values below those calculated for a fixed label. At small K, linearity allows us to treat this motion rigorously by convoluting the time-dependent sum and difference impulse response functions with the pump pulse. At larger K this becomes more difficult because the rotational diffusion equations governing the depletion of the ground-state distribution during the pump period would have to be solved.

Effects of Rapid Wobbling

Generally there will be some extremely rapid but restricted motions of the label at its binding site. These motions relax within nanoseconds or less, whereas typical pump durations last at least 100 ns. To qualitatively allow for these unresolvable motions, we use a wobble model where the label moves rapidly within a binding site that is considered to be fixed during the pump period. The observed rotational motions of the label then involve only the slower nonwobble motions of the surrounding binding site. We assume isotropic wobbling such that any vector fixed in the label is uniformly distributed within a cone of semiangle α. Then $\hat{\mu}_p$, $\hat{\mu}_a$, and $\hat{\mu}_e$ are distributed about three unit vectors fixed in the binding site that are denoted $\hat{\mu}_p^*$, $\hat{\mu}_a^*$, and $\hat{\mu}_e^*$, respectively. Rapid wobbling allows us to average any function of $\hat{\mu}_p$, $\hat{\mu}_a$, and $\hat{\mu}_e$ independently over the three cones involved. For a particular $\hat{\mu}_p$, $\hat{\mu}_a$, and $\hat{\mu}_e$; $P_2(\hat{\mu}_a \cdot \hat{\mathbf{p}})$ averages to $XP_2(\hat{\mu}_a^* \cdot \hat{\mathbf{p}})$ and $P_2(\hat{\mu}_e \cdot \hat{\mathbf{p}})$ averages to $XP_2(\hat{\mu}_e^* \cdot \hat{\mathbf{p}})$, where $X = 0.5\cos\alpha(1 + \cos\alpha)$. In addition, if ω denotes the orientation of axes fixed in the binding site, the initial distribution of binding sites surrounding ground-state labels remaining after the pump pulse, denoted $R^*(\hat{\mathbf{p}}, \mathbf{r}, \omega, 0)$, is given as

$$R^*(\hat{\mathbf{p}},\mathbf{r},\omega,0) = (n_0/8\pi^2)\exp[-Kf(\mathbf{r})\{1 + 2XP_2[\hat{\mu}_p^*(\omega)\cdot\hat{\mathbf{p}}]\}], \quad (18)$$

where n_0 is again the prepump concentration of the label. Integrating $R^*(\hat{\mathbf{p}}, \mathbf{r}, \omega, 0)$ over all ω gives the ground-state concentration $n(\mathbf{r}, 0)$ of the label. Note that $R^*(\hat{\mathbf{p}}, \mathbf{r}, \omega, 0) \rightarrow R(\hat{\mathbf{p}}, \mathbf{r}, \omega, 0)$ of Eq. 14 as $\alpha \rightarrow 0°$.

It can be shown from these results that r_a and r_e reduce simply to

$$r_a(t) = g_0X^2\langle P_2[\hat{\mu}_a^*(t)\cdot\hat{\mu}_p^*(0)]\rangle$$
$$r_e(t) = g_0X^2\langle P_2[\hat{\mu}_e^*(t)\cdot\hat{\mu}_p^*(0)]\rangle, \quad (19)$$

where g_0 is a simple constant discussed below and X^2 expresses the initial decrease in apparent anisotropy due to unresolvable wobbling. The time-dependent expectation values, as defined by Eq. 11, involve dot products between a binding site's vectors $\hat{\mu}_a^*$ and $\hat{\mu}_e^*$ at time t and $\hat{\mu}_p^*$ at $t = 0$ and express the slower, observable rotations of the label. Various dynamic models can be used to give explicit time-dependent expressions for the rotational relaxation. If the label is firmly bound such that wobbling can be ignored, then Eq. 19 reduces to Eq. 13 as $\alpha \rightarrow 0°$.

The initial constant g_0 can be defined by $g_0X\Delta S(0) = \Delta D_p(0)$, where

$$\Delta D_p(0) = 3q\int\int I(\mathbf{r})P_2(\hat{\mu}_p^*\cdot\hat{\mathbf{p}})\Delta R^*(\hat{\mathbf{p}}, \mathbf{r}, \omega, 0)d^3\mathbf{r}d^3\omega, \quad (20)$$

with $\Delta R^*(\hat{\mathbf{p}}, \mathbf{r}, \omega, 0) = n_0/8\pi^2 - R^*(\hat{\mathbf{p}}, \mathbf{r}, \omega, 0)$. Expanding $R^*(\hat{\mathbf{p}}, \mathbf{r}, \omega, 0)$ gives

$$\Delta S(0)/S_0 = sK[1 - (0.5 + 0.4X^2)s'K + \ldots]$$
$$\Delta D_p(0)/S_0 = (2/5)sKX[1 - (1 + 2X/7)s'K + \ldots], \quad (21)$$

and from this

$$g_0 = 2/5[1 - 0.5(1 + 4X/7 - 4X^2/5)s'K + \ldots], \quad (22)$$

which is again 2/5 for $K \ll 1$. The correction term depends on X and collapses to that in Eq. 17 when $X = 1$.

Eq. 21 shows that for $K \ll 1$, the fractional change in S is independent of the label's rotational mobility during the pump pulse and simply equal to sK. If s is known, then K can be determined in this regime regardless of any wobbling. However, even if K is quite large (saturation regime) small fractional changes in S can result if there is poor beam overlap. To set $g_0 = 2/5$, then $\Delta S(0)/S_0$ should not only be small but should also vary linearly as the pump pulse intensity or duration is varied over a small range.

DISCUSSION

The sensitivity and selectivity of fluorescent labels makes them ideal probes of macromolecular rotational dynamics. On nanosecond time scales, fluorescence depolarization can give details about rotations of the smaller proteins. On longer time scales appropriate to larger macromolecules, macromolecular complexes and assemblies, several more recent techniques can be used. These include fluorescence correlation spectroscopy (FCS) discussed by Ehrenberg and Rigler (1974, 1976) and Aragon and Pecora (1975, 1976) that monitors spontaneous fluctuations and FRS discussed here that monitors relaxation following an initial perturbation. Both FCS and FRS use a probe beam to generate a fluorescence signal that reflects the instantaneous state of the sample if all other correlation times involved are long compared with the fluorescence lifetime. The signal involves both absorption and emission, so that general FRS and FCS expressions are necessarily more complicated than those of other optical techniques, such as luminescence depolarization, which involves only the emission process, or linear dichroism, which involves only the absorption process. However, this dual dependence also means that the information content available in FRS and FCS is greater than that in either of these other techniques.

In this paper, we described several FRS setups for solution studies that simplify the analysis considerably by eliminating the dependence on either the absorption dipole stimulated by the probe beam or the dipole governing the

reemission of fluorescence. Combinations of parallel and perpendicular polarization alignments allowed two anisotropy functions to be formed that separately involved the rotational motions of either dipole. In cases of isotropic rotations, both anisotropy functions give the same results up to an initial value. In highly anisotropic systems, however, the results can be very different, provided that the transition dipoles involved have different directions in the label's molecular axes. Both anisotropy functions also involved the absorption dipole excited by the pump. The usefulness of FRS will be further realized if wavelength-tunable probe and pump beams can be used to excite different transition directions in the label. In recent nanosecond fluorescence depolarization studies, Barkley et al. (1981) demonstrated how anisotropy functions obtained at different wavelengths and temperatures can be used to investigate anisotropic rotations of small molecules. Their method of analysis could also be applied to larger rigid macromolecular systems probed by FRS setups described here.

Johnson and Garland (1981) used microscope optics in their FRS study to look at the rotational motions of band 3 protein in erythrocyte membranes. They found rotations appearing faster in oriented systems than in randomly oriented systems. How well their interpretations of these results apply is unclear, because special precaution was not taken to ensure that their signal involved only the absorption dipole excited by the probe beam or the emission dipole for fluorescence. In general, an FRS signal with some dual dependence will contain additional higher order rotational relaxation terms that decay at a faster rate. For a label rigidly fixed to a sphere of diffusion coefficient D, there will be an $\exp(-20Dt)$ term present besides the $\exp(-6Dt)$ term. The magnitude of complicating faster terms may have been minimized in their optical system. However, FRS setups for solution studies described here or employing 2π or 4π collection optics are specifically designed to eliminate these additional terms and provide a tractable quantitative treatment of rotational dynamics.

The author would like to thank Professor Rudolf Rigler for his support and encouragement during the author's stay in the Department of Medical Biophysics at the Karolinska Institute, Stockholm, Sweden.

The initial portion of this work in Stockholm was supported by a Swedish Medical Research Postdoctoral Fellowship awarded to the author. The completion of this work in Dallas was supported by National Institutes of Health grants HL268812 and GM32437.

Received for publication December 1983 and in final form 15 June 1984.

REFERENCES

Aragon, S. R., and R. Pecora. 1975. Fluorescence correlation spectroscopy and Brownian rotational diffusion. *Biopolymers.* 14:119–138.

Aragon, S. R., and R. Pecora. 1976. Fluorescence correlation spectroscopy as a probe of molecular dynamics. *J. Chem. Phys.* 64:1791–1803.

Austin, R. H., S. S. Chan, and T. M. Jovin. 1979. Rotational diffusion of cell surface components by time-resolved phosphorescence anisotropy. *Proc. Natl. Acad. Sci. USA.* 76:5650–5654.

Barkley, M. D., A. A. Kowalczyk, and L. Brand. 1981. Fluorescence decay studies of anisotropic rotations of small molecules. *J. Chem. Phys.* 75:3581–3593.

Belford, G. G., R. L. Belford, and G. Weber. 1972. Dynamics of fluorescence polarization in macromolecules. *Proc. Natl. Acad. Sci. USA.* 69:1392–1393.

Cherry, R. J. 1979. Rotational and lateral diffusion of membrane proteins. *Biochim. Biophys. Acta.* 559:289–327.

Cherry, R. J., and R. E. Godfrey. 1981. Anisotropic rotation of bacteriorhodopsin in lipid membranes. Comparison of theory with experiments. *Biophys. J.* 36:257–276.

Cherry, R. J., E. A. Nigg, and G. S. Beddard. 1980. Oligosaccharide motion in erythrocyte membranes investigated by picosecond fluorescence polarization and microsecond dichroism of an optical probe. *Proc. Natl. Acad. Sci. USA.* 77:5899–5903.

Chung, T. J., and K. B. Eisenthal. 1972. Theory of fluorescence depolarization by anisotropic rotational diffusion. *J. Chem. Phys.* 57:5094–5097.

Ehrenberg, M., and R. Rigler. 1972. Polarized fluorescence and rotational Brownian motion. *Chem. Phys. Lett.* 14:539–544.

Ehrenberg, M., and R. Rigler. 1974. Rotational Brownian motion and fluorescence intensity fluctuations. *Chem. Phys.* 4:390–401.

Ehrenberg, M., and R. Rigler. 1976. Fluorescence correlation spectroscopy applied to rotational diffusion of macromolecules. *Q. Rev. Biophys.* 9:69–79.

Hogan, M., J. Wang, R. H. Ausin, C. L. Monitto, and S. Hershkowitz. 1982. Molecular motion of DNA as measured by triplet anisotropy decay. *Proc. Natl. Acad. Sci. USA.* 79:3518–3522.

Johnson, P., and P. B. Garland. 1981. Depolarization of fluorescence depletion. A microscopic method for measuring rotational diffusion of membrane proteins on the surface of a single cell. *FEBS (Fed. Eur. Biochem. Soc.) Lett.* 132:252–256.

Jovin, T. M., M. Bartholdi, W. L. C. Vaz, and R. H. Austin. 1981. Rotational diffusion of biological macromolecules by time-resolved delayed luminescence (phosphorescence, fluorescence) anisotropy. *Ann. NY Acad. Sci.* 366:176–196.

Kinosita, K., Jr, S. Kawato, and A. Ikegami. 1977. A theory of fluorescence polarization decay in membranes. *Biophys. J.* 20:289–305.

Peters, R. 1981. Mini-review. Translational diffusion in the plasma membrane of single cells as studied by fluorescence microphotolysis. *Cell Bio. Int. Reports.* 5:733–760.

Smith, L. M., R. M. Weis, and H. M. McConnell. 1981*a*. Measurement of rotational motion in membranes using fluorescence recovery after photobleaching. *Biophys. J.* 36:73–91.

Smith, L. M., H. M. McConnell, B. A. Smith, and J. W. Parce. 1981*b*. Pattern photobleaching of fluorescent lipid vesicles using polarized laser light. *Biophys. J.* 33:139–146.

Strambini, G. B., and W. C. Galley. 1980. Time-dependent phosphorescence anisotropy measurements of the slow rotational motions of proteins in viscous solution. *Biopolymers.* 19:383–394.

Wahl, Ph. 1975. Decay of fluorescence anisotropy. *In* Biochemical Fluorescence Concepts. Vol. 1. R. F. Chen and H. Edelhoch, editors. Marcel Dekker, Inc., New York. 1–41.

Wang, J., M. Hogan, and R. H. Ausin. 1982. DNA motions in the nucleosome core particle. *Proc. Natl. Acad. Sci. USA.* 79:5896–5900.

Wegener, W. A., and R. Rigler. 1984. Separation of translational and rotational contributions in solution studies using fluorescence photobleaching recovery. *Biophys. J.* 46:787–793.